Practical Active Control System for Combustion Oscillations

P. J. Langhorne*
University of Otago, Dunedin, New Zealand
and
A. P. Dowling† and N. Hooper‡
Cambridge University, Cambridge, England, United Kingdom

A low-frequency combustion instability of a flame burning in a duct has been successfully controlled by the unsteady addition of extra fuel. A suitably phased addition of only 3% more fuel reduces the peak in the pressure spectrum due to the combustion instability by some 12 dB. The acoustic energy in the 0–400 Hz bandwidth is reduced to 18% of its uncontrolled value. Since relatively little unsteady fuel is necessary, the mechanical power requirements of the controller are modest and the system is easy to implement.

Nomenclature

$c(x)$ = sound speed
$G(\omega)$ = transfer function across the feedback circuit
$I(x,t)$ = light emission from a 75-mm length of ducting centered on x
k = $\bar{P}_{\text{inj}}/V_o$
L = duct length
M_1 = mass flow rate of primary premixed air = $m_{a1} + m_{f1}$
M_2 = mass flow rate of secondary premixed air = $m_{a2} + m_{f2}$
m_{a1} = mass flow rate of primary air
m_{a2} = mass flow rate of secondary air
m_{f1} = mass flow rate of primary fuel
m_{f2} = mass flow rate of secondary fuel
$\bar{P}_{\text{inj}}$ = $\bar{p}_{\text{inj}}/210$ kPa
$p(x,t)$ = pressure
$p_{\text{inj}}(t)$ = pressure in feed ring supplying fuel injectors
$p_{\text{ref}}(t)$ = pressure perturbation at reference position $x = 0.725$ m
$Q(x,t)$ = heat release rate in 75-mm length of ducting centered on x
$q(x,t)$ = heat release rate/unit length
$S_p(\omega)$ = power spectral density of $p_{\text{ref}}(t)$
$S_{pQ}(\omega)$ = cross-power spectral density of $p(x,t)$ and $Q(x,t)$
$T(\omega)$ = transfer function between p_{ref} and v for $v_0 = 0.5$ V, $\bar{p}_{\text{inj}} = 210$ kPa
$T_E(\omega)$ = experimental measurements of $T(\omega)$
t = time
V_o = $v_o/0.5$ V
$v(t)$ = input voltage to injectors
v_o = amplitude of input voltage to injectors
x = axial distance downstream of choked nozzle
γ = ratio of specific heat capacities
δ = decay rate of linear disturbances
Δp = gauge pressure upstream of flame
$\rho(x,t)$ = density
τ = time delay across the feedback circuit
ϕ_1 = equivalence ratio of primary gas
ϕ_2 = equivalence ratio of secondary gas
ϕ_T = total mean equivalence ratio
ω = frequency
ω_{Ej} = frequencies at which $T(\omega)$ is measured, $j = 1,2,\ldots,$

Superscripts
$\bar{}$ = mean
$'$ = perturbation
$\hat{}$ = Fourier transform
$*$ = complex conjugate

Received June, 29, 1988; revision received March 29, 1989.

*Lecturer, Department of Physics.
†Reader, Department of Engineering.
‡Reader, Department of Engineering.

Introduction

WHEN combustion takes place within an acoustic resonator, the interaction between acoustic waves and unsteady combustion may lead to oscillations of damaging intensity. Such a combustion instability can occur in the afterburners of jet aeroengines, where it has a low frequency and is termed "reheat buzz." Similar oscillations have been observed on laboratory rigs in which a flame burns in the wake of a bluff body in a duct. There schlieren photographs (see for example, Smart et al.[1]) show that the flame is perturbed by velocity fluctuations at the flameholder, which alter the instantaneous heat-release rate. If this unsteady heat-release rate is in phase with local pressure perturbations, Rayleigh's criterion[2] states that the disturbances will grow. Longitudinal pressure waves propagating in the duct can then become destructively large in magnitude. Since passive dampers are ineffective at these low frequencies, the traditional solution has been to modify the aerodynamics of the burner to reduce the coupling between the heat-release rate and the unsteady flow. However, there are frequently constraints on burner/flame-stabilizer design and the only alternative is to limit the heat release in the duct. In afterburners, this means that a limit is placed on the available thrust.

A low-frequency combustion instability in a duct lends itself to the techniques of active control. In this, a feedback signal taken from the unstable system is suitably processed and used to drive an actuator so as to reduce the instability. This may be done either by changing the boundary conditions so that more energy is lost at the boundaries or by altering the unsteady heat-release rate so that the energy gain is reduced.

There have now been a number of demonstrations of the success of active control techniques in suppressing combustion instabilities on laboratory-scale apparatus. One of the simplest of these is the Rijke tube.[2] This is a vertical pipe, open at both ends, which contains a heated gauze or a flame. Such a pipe has a natural, half-wave resonance. The perturbations associated with this resonance induce fluctuations in the heat-release rate that lag the unsteady velocity. Thus, when the heat source is in the lower half of the pipe, the unsteady pressure and heat-release rate are in phase and, according to Rayleigh's criterion, any linear perturbations will grow. The pressure fluctuations are sinusoidal with little cycle-to-cycle variation and it is possible to use active control to reduce the oscillations

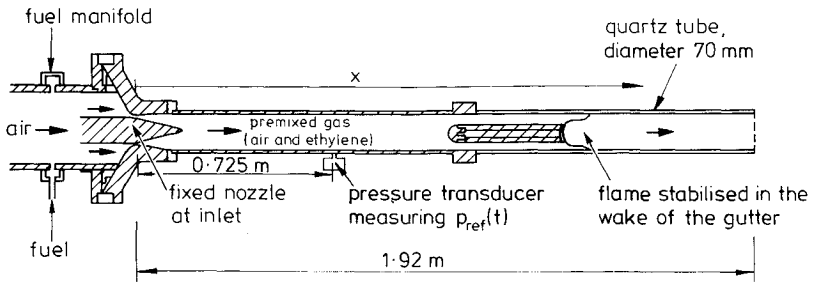

Fig. 1 Reheat buzz rig (not to scale).

to negligible levels. This has been carried out in two different ways. Collyer and Ayres,[3] Heckl,[4] and Screenivasan et al.[5] introduced a second controlling heat source into the upper half of the tube. The unsteady heating associated with this second heat source is out of phase with the pressure perturbations and dampens any oscillations. Alternatively, Dines[6] altered the energetics of linear perturbations by actively modifying the boundary condition at the end of the tube using a loudspeaker. The feedback signal here was the light emission from CH radicals in the flame, which has been shown to be a measure of heat-release rate.[7] Heckl[8] has achieved noise reduction in essentially the same way as Dines, but using pressure fluctuations as the feedback signal to the loudspeaker.

In addition to the work on the Rijke tube, combustion instabilities have been controlled on other small-scale apparatus. Kidin et al.[9] have used a novel technique for generating the controlling pressure fluctuations, the expansion from a dc discharge. More conventional methods, very similar to Heckl's, were used on a 1 kW laminar premixed burner by Lang et al.[10] They restated the encouraging observation for the application of active control techniques to practical devices that the energy consumption of the controller is very small.

Consequently, Poinsot et al.[11] progressed to a more realistic and practical burner. The apparatus is a diffusion turbulent combustor with an airflow rate of 0.024 kg/s^{-1} and a fuel-to-air ratio which is 40% of the stoichiometric value for propane. Pressure oscillations were sensed by a microphone, suitably filtered, delayed, amplified, and fed into a pair of loudspeakers. At the frequency of the combustion oscillation, the uncontrolled peak of 125 dB was reduced by 24 dB by the application of their control system.

Active control techniques have also been used successfully on a laboratory rig designed to model some of the essential features of the reheat system of a jet aeroengine.[12,13] The rig is illustrated in Fig. 1 and has been described in detail in Ref. 14. Air and ethylene are introduced at constant mass flow rates upstream of a choked nozzle. The gases mix as they enter the working section so that there is a uniform fuel-to-air ratio across the duct. The experiments of Bloxsidge and others were performed with a premixed mass flow rate of 0.135 kgs^{-1} (i.e., about 27 ms^{-1} upstream of the flameholder) and a fuel-to-air ratio of 66% of the stoichiometric ratio. The premixed flame is stabilized in the wake of a conical gutter and undergoes an acoustically coupled combustion instability called "buzz." Control was applied by actively changing the boundary condition at the upstream end of the working section. In these experiments, the fixed nozzle was replaced by a moveable one. The mass flow rate of premixed gas entering the working section could then be changed by altering the axial position of this nozzle, thereby modifying the upstream boundary condition. The nozzle was driven by a suitably processed pressure signal from the rig. Once implemented, the 162-dB peak in the pressure spectrum due to the buzz was reduced by 20 dB. In addition, the acoustic energy in the bandwidth 0–800 Hz was diminished to 10% of its value without control. Furthermore, the modified "buzz" frequency and modal pressure distribution with control were successfully predicted using the calculations described by Bloxsidge et al.[15]

Although this method of control was successful on a 0.25-MW turbulent premixed burner with significant cycle-to-cycle variations, the method of implementation is not a practical proposition for full-scale afterburners. Likewise, it is impractical to consider the use of loudspeakers to produce significant pressure fluctuations in environments where mass flows of many kilograms per second are to be handled. In this paper, we describe the results of a series of experiments to investigate a more practical means of implementing the feedback. The basic rig is identical to that used by Bloxsidge et al. (and illustrated in Fig. 1), but control is achieved by the unsteady addition of fuel near the flameholder. We exploit the fact that unsteady combustion is very effective at producing high-intensity sound levels. The pressure perturbation measured by a transducer upstream of the flame will be the input to the control circuit. The idea of the control is to use fast-response solenoid valves to pulse fuel into the rig in response to this input. This produces an additional unsteady rate of heat release which, if the control circuit is suitably designed, stabilizes the flame.

Practical Control System

The use of unsteady addition of fuel as a means of controlling combustion instabilities has been tested on the rig illustrated in Fig. 1. In the basic configuration, the fuel (ethylene) and air are introduced at constant mass flow rates upstream of a nozzle. This nozzle is choked to ensure that the supplies of fuel and air are acoustically isolated from the working section. The ethylene and air mix well in the constriction and enter the working section as a premixed gas. The working section is just a straight duct in which a flame is stabilized in the wake of a conical gutter. The experiments were performed with a premixed mass flow rate of 0.135 kgs^{-1} and equivalence ratios (defined as the ratio of mass of fuel to mass of air as a fraction of the ratio required for stoichiometric burning) in the range 0.63–0.70. We measure the pressure perturbation $p'(x,t)$ at various axial distances x downstream of the choked nozzle. In addition, the light emission from short-lived C_2 radicals in the flame is monitored. The optical arrangement is straightforward. A screen blanks off all but a 75-mm length of flame. An image of this portion is focused through a filter chosen pass the light emitted in the main C_2 transition, and onto the photocathode of a photomultiplier. Two nominally identical systems are available, with filters centered on 516.7 and 518.0 nm of bandwidth 3.2 and 3.6 nm, respectively. $I(x,t)$ denotes the output from the photomultiplier for the window centered on x. Hurle et al.[7] have shown that, under certain conditions, the heat-release rate is proportional to this light emission. Previous work[14,15] has shown that this is a valid assumption for this apparatus under limited conditions. A measurement of the stagnation temperature rise across the duct length therefore enables the photomultiplier output in volts to be converted into heat-release rate. We denote the heat-release rate in the window centered on x by $Q(x,t)$, which may be decomposed into its mean and fluctuating components, $\bar{Q}(x)$ and $Q'(x,t)$, respectively.

The combustion oscillations in this rig have significant cycle-to-cycle variations, and if they are to be successfully con-

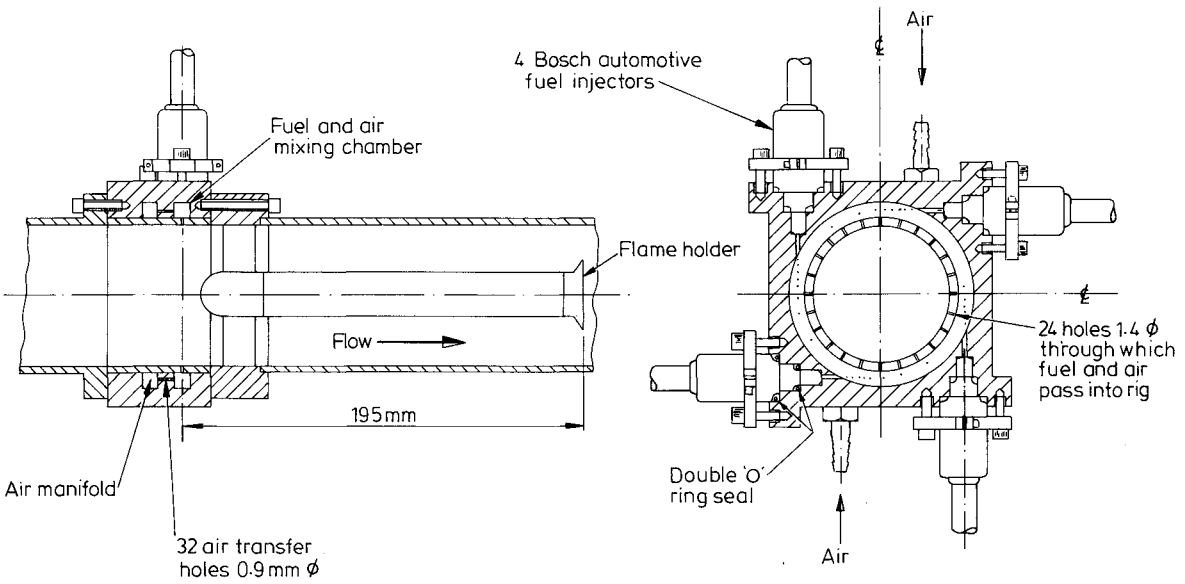

Fig. 2 Detail of mixing device for the secondary fuel and air.

trolled by feedback, the time delay in the feedback system must be kept as short as possible. In earlier work, Bloxsidge and others noted that an additional time delay of one cycle (about 13 ms) led to a 10-dB degradation in the performance of the controller. We aim to use the fluctuations in heat-release rate due to imposed variations in fuel-air ratio as our control. These nonuniformities will convect with the fluid from the solenoid valves to the flame. The primary fuel manifold is so far upstream of the flame in our premixed rig that the time delay between the primary injection of fuel and its combustion is prohibitively large. Consequently, when implementing the control the primary supplies of fuel and air are kept steady and a secondary unsteady supply of fuel is introduced close to the flameholder.

We chose to use automotive fuel injectors to pulse this secondary fuel. These direct-acting solenoid valves are cheap, robust, and readily available. Design calculations showed that four injectors were required to provide sufficient fuel flow rate to control the instability. They have the advantage of being electrically operated with a response time of less than 1 ms.[16] Their disadvantage is that they have only two modes of operation: they are either fully opened or closed. The delivered mass flow of fuel depends both on the pressure in the supply feeding the injectors and on the length of time they are open, and is related to the input voltage in a nonlinear way.

The addition of a secondary supply of neat fuel in premixed gas at a location close to the flame will create local rich spots and destabilize the flame. We must therefore ensure that the secondary fuel is well mixed with air before it is incident on the flame. Consequently, air is added to the secondary fuel in a chamber prior to injection into the rig (see Fig. 2). Rapid and complete mixing is required in this chamber. Air flows steadily into the chamber while the fuel enters unsteadily through the choked injectors. The two streams meet in perpendicular directions to maximize mixing. If the control is to be effective, the mixing chamber must be flushed in a fraction of a cycle. This time is estimated to be about 2 ms. This time delay and the opening time of the injectors are small in comparison with the time taken for the secondary fuel to convect along the working section to the flameholder. This is of the order of 7 ms, or half a cycle at a typical frequency of the combustion instability. The delay represents a reasonable compromise between the conflicting requirements of minimizing the time delay while ensuring that the jets of secondary gas enter the working section sufficiently far upstream of the combustion zone to prevent the flame from stabilizing in their wakes.

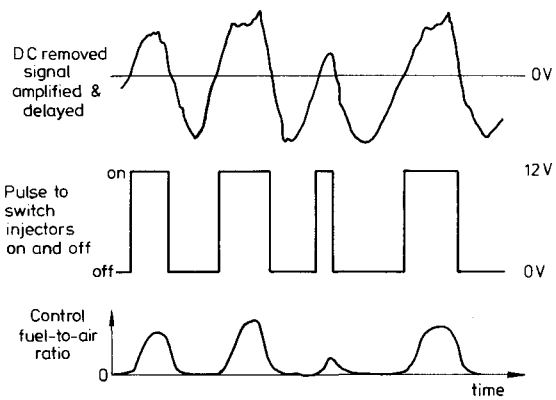

Fig. 3 Control system.

It is worth noting that the requirement of a secondary fuel and air supply for control is peculiar to a premixed rig and would not apply to an afterburner. There the primary fuel is injected sufficiently close to the combustion region for modulations in this fuel flow rate to be used for control.

An unsteady signal is taken from the rig and used as input to the control circuit. The main criterion for the choice of control signal is that it should have a large signal-to-noise ratio at the buzz frequency. The unsteady light emission from C_2 radicals close to the exit of the duct and a pressure upstream of the region of combustion have both been successfully used as control signals. The dc component is removed from this unsteady signal. It is then amplified and a suitable time delay is imposed (see Fig. 3). When this voltage is positive, the injectors are opened. The secondary air enters the rig steadily and continuously so that the fuel-to-air ratio of secondary gas is varied.

In the experiments to be described in this paper, the primary mass flow of premixed gas M_1 and primary equivalence ratio ϕ_1 are set to produce a flame of the required stability. Secondary air flows steadily into the rig with a mass flow rate m_{a2} which is unchanged throughout all of the experiments. The mass flow of secondary fuel m_{f2} not only depends on the proportion of a cycle over which the injectors are open, but also on the pressure in a feed ring joining the inlets of the four injectors denoted by p_{inj}. The slow response of the pressure regulator controlling p_{inj} means that it decreases whenever the injectors are open and rises again as they are shut. We will

denote the mean of p_{inj} by $\bar{p}_{inj}$. The secondary mass flow M_2 and its equivalence ratio $\phi_2 = \bar{\phi}_2 + \phi_2'$ can be altered in the following four ways:

1) The injectors are closed and there is no secondary fuel flow m_{f2}, so that $\phi_2 = 0.0$.

2) The injectors are held open so that m_{f2} is steady and $\phi_2 = \bar{\phi}_2$ with no unsteady component ϕ_2'.

3) The injectors are driven by the signal from a function generator at a range of frequencies so that m_{f2} and $\phi_2 = \bar{\phi}_2 + \phi_2'$ have a mean component and unsteady component of constant amplitude.

The injectors are driven from a feedback signal from the rig so that $\phi_2 = \bar{\phi}_2 + \phi_2'$, where the magnitude of both the mean and unsteady components depends on the effectiveness of the control.

Under all four types of conditions, the premixed gas downstream of the secondary supply will have a total mean equivalence ratio ϕ_T associated with it, where

$$\phi_T = \frac{m_{f1} + \bar{m}_{f2}}{(m_{a1} + m_{a2}) \times 0.068}$$

ϕ_T can therefore be increased by an increase in either ϕ_1 or $\bar{\phi}_2$.

Information to aid in the design of the control circuit can be obtained by driving the injectors as in (3) to obtain the transfer function between $v(t)$, the input voltage to the injectors, and the control signal, which is chosen in what follows as the pressure perturbation at $x = 0.725$ m and will be denoted by $p_{ref}(t)$. The nonlinear element of our actuator is that the fuel injectors are either open or closed. They open whenever the input voltage is positive. Consider a sinusoidal input $v(t) = v_o \sin \omega t$. The form of the nonlinearity in the behavior of the fuel injectors means that the fuel flow rate and hence the burning rate and pressures generated in the rig are independent of v_o. Moreover, since the fuel injectors are choked throughout their practical operating range, the flow rate is directly proportional to $\bar{p}_{inj}$, the mean back pressure supplied to the injectors. Diffusion between the fuel addition and its combustion attenuates the effect of high-frequency pulsations in fuel, and so it is enough just to consider the fundamental component of $p_{ref}(t)$. Since $\hat{p}_{ref}(\omega)$ is independent of v_o and directly proportional to $\bar{p}_{inj}$, we can write the transfer function $\hat{p}_{ref}(\omega)/\hat{v}(\omega)$ in the form

$$\frac{\hat{p}_{ref}(\omega)}{\hat{v}(\omega)} = \frac{\bar{p}_{inj}}{v_o} S(\omega) \tag{1}$$

where S is independent of both v_o and $\bar{p}_{inj}$.

Once $S(\omega)$ is known, describing-function analysis (see for example, Ogata[17]) may be used to calculate the required characteristics of the control circuit. Usually, this transfer function would be determined at the running condition of interest by applying a sinusoidal input voltage for a range of frequencies ω and measuring the response. Unfortunately, such a procedure is not possible here because the system to be controlled is unstable and the instability swamps any response to an imposed input voltage. Instead, we run the rig at a low equivalence ratio at which the flame/duct arrangement is stable and measure the transfer function $T(\omega) = \hat{p}_{ref}(\omega)/\hat{v}(\omega)$. This transfer function is then extended analytically to give a form for $T(\omega)$ at the higher fuel-air ratios at which the system is unstable. This may then be used to design a suitable feedback circuit. The theory will assume that the only nonlinearity in the system is that due to the on-off behavior of the fuel injectors. Any nonlinearity in the response of the duct/flame arrangement is therefore neglected.

Figure 4 shows the measured response $T(\omega)$ to forcing at various frequencies for $v_0 = 0.5$ V, $\bar{p}_{inj} = 210$ kPa, and an equivalence ratio ϕ_1 of 0.63 at which the flame is stable. The experimental measurements of the transfer function $T_E(\omega)$ were obtained at 14 different frequencies, ω_{Ej}, $j = 1,\ldots,14$. We seek to fit an analytical expression to these measured transfer functions.

Consider a time dependence proportional to $e^{i\omega t}$. Since the flames is stable, we know that $T(\omega)$ has a pole in the upper half ω plane and denote its position by $\omega_R + i\delta$. The δ is positive and describes the decay rate of linear disturbances. The transfer function may therefore be expressed as

$$T(\omega) = \frac{F_1(\omega)}{\omega - \omega_R - i\delta} \tag{2}$$

where $F_1(\omega)$ has yet to be determined. However, since $T(\omega)$ is the transfer function between two real quantities, $T(-\omega) = T^*(\omega)$ where the asterisk denotes a complex conjugate, and it is more natural to write

$$T(\omega) = \frac{F_2(\omega)}{(\omega - \omega_R - i\delta)(\omega + \omega_R - i\delta)} \tag{3}$$

The data shown in Fig. 4 demonstrate a change in the phase of the transfer function with frequency such as that due to a constant time delay. This can be displayed explicitly by expanding $T(\omega)$ in the form

$$T(\omega) = \frac{F_3(\omega) e^{-i\omega\beta}}{(\omega - \omega_R - i\delta)(\omega + \omega_R - i\delta)} \tag{4}$$

If we assume $F_3(\omega)$ to be a slowly varying function of frequency, for all ω near ω_R, $T(\omega)$ can be written as

$$T(\omega) = \frac{A e^{-i\omega\beta}}{(\omega - \omega_R - i\delta)(\omega + \omega_R - i\delta)} \tag{5}$$

where $A = F_3(\omega_R)$ is a complex number. Similarly, for ω near $-\omega_R$, we have

$$T(\omega) = \frac{A^* e^{-i\omega\beta}}{(\omega - \omega_R - i\delta)(\omega + \omega_R - i\delta)} \tag{6}$$

since $A^* = F_3(-\omega_R)$.

We are primarily interested in $T(\omega)$ in the vicinity of its poles, since it is its behavior there that determines the required characteristics of the feedback circuit. We will therefore take the form of $T(\omega)$ in Eq. (5) for all positive real ω, and the form in Eq. (6) for negative real ω. The constants $A (= A_R + iA_I)$, β, ω_R, and δ in this expression are to be found by minimizing the sum of squares of the errors between the analytical and

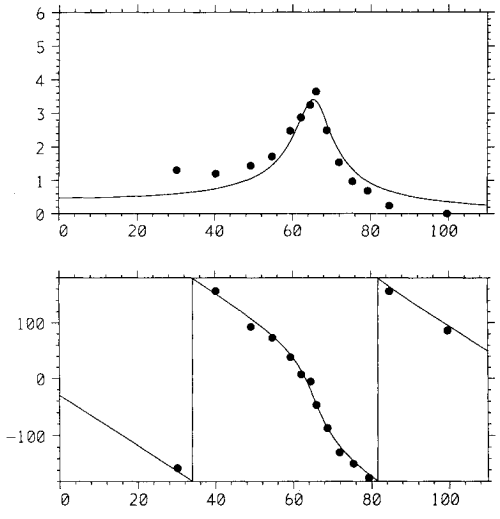

Fig. 4 Comparison of analytical and experimental transfer functions for $\phi_1 = 0.63$, $v_o = 0.5$ V, and $\bar{p}_{inj} = 210$ kPa. •: experimental transfer function $T_E(\omega)$; and ——: analytical transfer function $T(\omega)$ of the form given in Eq. (5) with $A = (-7.02 + i4.00)10^4$ kPa/Vs^2, $\beta = 11.8$ ms, $\omega_R = 411$ rad^{-1}, and $\delta = 28.8$ s^{-1}.

experimental transfer function, i.e., by minimizing

$$\sum_{j=1}^{14} |T(\omega_{Ej}) - T_E(\omega_{Ej})|^2$$

The minimization was performed by NAG routine E04FNF and the constants found to be $A = (-7.02 + i4.00)10^4$ kPa/Vs^2, $\beta = 11.8$ ms, $\omega_R = 411$ rad^{-1}, and $\delta = 28.8$ s^{-1}. This theoretical transfer function is compared with measurements in Fig. 4. The agreement is good near the resonant peak, but the magnitude of the transfer function at low frequencies is somewhat underestimated. This is not surprising since no attempt was made to describe $T(\omega)$ at these low frequencies. When the Nyquist stability criterion is applied, these low frequencies lead to curves close to the origin with little effect on the stability threshold.

The resonant frequency ω_R and the damping δ are strong functions of fuel-to-air-ratio, but we hypothesize that A and β only vary slowly. If this were true, they could be treated as fixed constants for modest changes in equivalence ratio. This supposition was tested by measuring the transfer function $T_E(\omega)$ at a different equivalence ratio $\phi_1 = 0.65$ with $v_0 = 0.5$ V and $\bar{p}_{inj} = 210$ kPa as before. The measurements are displayed in Fig. 5. Once again a theoretical expression of the form in Eq. (5) was fitted to these measurements, but now A and β were kept fixed at the values determined from the $\phi_1 = 0.63$ data. The function

$$\sum_{j} |T(\omega_{Ej}) - T_E(\omega_{Ej})|^2$$

was minimized by varying ω_R and δ only. The best fit was found to be for $\omega_R = 450$ rad^{-1} and $\delta = 17.3$ s^{-1}. Figure 5 shows the comparison between this theoretical transfer function and the measurements. The agreement is very encouraging.

The control was applied to a case with equivalence ratio $\phi_1 = 0.68$. The flame/duct arrangement is then unstable with small oscillations growing into a nonlinear limit cycle of frequency 74 Hz. Theoretical work on this combustion instability[15] has shown that there is little difference between the frequency of the unstable linear system and the nonlinear limit cycle frequency. We therefore take $\omega_R = 465$ rad^{-1} for this running condition. Since linear disturbances grow, δ must be negative at this equivalence ratio. The precise value of δ is not known at this stage and so we will investigate the feedback required for various values of δ. Ironically, once the instability has been controlled, δ can be determined by switching off the control and measuring the growth rate of small-amplitude disturbances.

Equation (1) describes how $T(\omega)$, the transfer function for $v_o = 0.5$ V and $\bar{p}_{inj} = 210$ kPa, should be modified to describe $\hat{p}_{ref}(\omega)/\hat{v}(\omega)$ for arbitrary values of v_o and $\bar{p}_{inj}$. It shows that in general

$$\frac{\hat{p}_{ref}(\omega)}{\hat{v}(\omega)} = T(\omega)\frac{\bar{P}_{inj}}{V_o} \tag{7}$$

where V_o and $\bar{P}_{inj}$ are v_o and $\bar{p}_{inj}$ normalized with respect to their values in the forcing experiments, i.e., $V_o = v_o/0.5$ V, $\bar{P}_{inj} = \bar{p}_{inj}/210$ kPa.

Consider applying negative feedback $G(\omega)$. Then

$$\hat{v}(\omega) = -G(\omega)\,\hat{p}_{ref}(\omega) \tag{8}$$

Since we already have $\hat{p}_{ref}(\omega) = \hat{v}(\omega)\,T(\omega)\,\bar{P}_{inj}/V_o$, these two conditions can be combined into a statement that

$$\hat{v}(\omega)\,[1 + G(\omega)\,T(\omega)\,\bar{P}_{inj}/V_o] = 0 \tag{9}$$

The natural frequencies of the system are the zeros of $[1 + G(\omega)\,T(\omega)\,\bar{P}_{inj}/V_o]$. If $[1 + G(\omega)\,T(\omega)\,\bar{P}_{inj}/V_o]$ has no zeros in the lower half ω plane, disturbances decay. We wish to keep the feedback circuitry as simple as possible and will

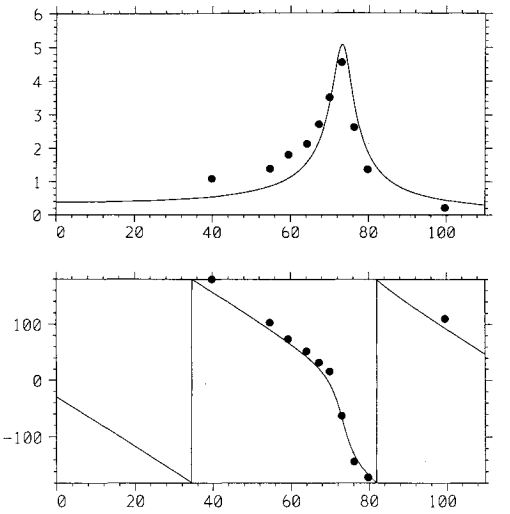

Fig. 5 Comparison of analytical and experimental transfer functions for $\phi_1 = 0.65$, $v_o = 0.5$ V, and $\bar{p}_{inj} = 210$ kPa. •: experimental transfer function $T_E(\omega)$; and ——: analytical transfer function $T(\omega)$ of the form given in Eq. (5) with $A = (-7.02 + i4.00)10^4$ kPa/Vs^2, $\beta = 11.8$ ms, $\omega_R = 460$ rad^{-1}, and $\delta = 17.3$ s^{-1}.

consider it to be made up only of a time delay, i.e.,

$$G(\omega) = -e^{-i\omega\tau} \tag{10}$$

where τ is real and positive.

Substitution for $T(\omega)$ and $G(\omega)$ from Eqs. (5) and (10) shows that the zeros of $[1 + G(\omega)\,T(\omega)\,\bar{P}_{inj}/V_o]$ are at

$$1 - \frac{A\bar{P}_{inj}e^{-i\omega(\beta+\tau)}}{V_o(\omega - \omega_R - i\delta)(\omega + \omega_R - i\delta)} = 0 \tag{11}$$

for Re $\omega > 0$. When $\bar{P}_{inj}/V_o$ is small and equal to k, say, this equation may be solved by an expansion in powers of k. To lowest order in k, there is a root at $\omega_R + i\delta$. Since δ is negative, this natural mode grows in time and is unstable. To first order in k, the natural frequency is

$$\omega_R + i\delta + \frac{Ak}{2\omega_R}e^{(\delta - i\omega_R)(\beta+\tau)}$$

The feedback shifts the frequency by $Ak\exp[(\delta - i\omega_R)(\beta+\tau)]/2\omega_R$. This reduces the growth rate and so has a stabilizing influence if the imaginary part of $Ak\exp[(\delta - i\omega_R)(\beta+\tau)]/2\omega_R$ is positive. With A rewritten as $|A|e^{i\alpha}$, this condition reduces to

$$2n\pi < \alpha - \omega_R(\beta+\tau) < (2n+1)\pi \tag{12}$$

for some integer n. For a given value of k, the feedback has the maximum stabilizing effect if the shift in frequency is purely imaginary; that is, if

$$\alpha - \omega_R(\beta+\tau) = \left(2n + \frac{1}{2}\right)\pi \tag{13}$$

Substitution for the values of α, ω_R, and β shows the minimum value of τ that satisfies Eq. (13) to be 4.0 ms. This time delay in the feedback circuit has the maximum stabilizing effect for small values of k. However, it is apparent from Eq. (12) that the feedback has some stabilizing influence for all values of τ in the range $0.6 < \tau < 7.3$ ms.

This approximate analysis only shows the trends for small levels of k. Describing-function analysis[17] may be used to determine the closed-loop stability more precisely. The locus of the points Re$[G(\omega)T(\omega)]$ vs Im$[G(\omega)T(\omega)]$ is plotted for real ω. It follows from complex variable theory[18] that the number

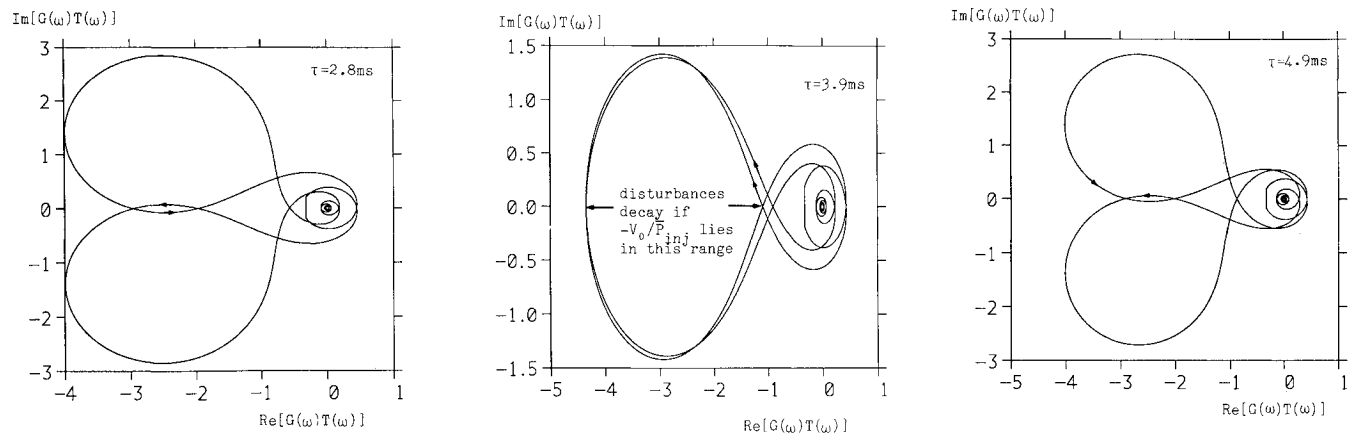

Fig. 6 Nyquist curves for various values of τ, the time delay across the feedback circuit, for $\delta = -20\ s^{-1}$.

of times this curve encircles $(-V_o/\bar{P}_{inj},0)$ clockwise is equal to the number of zeros minus the number of poles of $[1+G(\omega)T(\omega)\bar{P}_{inj}/V_o]$ in the lower half ω plane. Equations (5) and (6) show that $T(\omega)$ has two poles in the lower half ω plane. Hence, the criterion shows that the Nyquist curve must encircle the point $(-V_o/\bar{P}_{inj},0)$ twice anticlockwise for disturbances to decay.

Figure 6 shows the locus of the curve $\mathrm{Re}[G(\omega)T(\omega)]$ vs $\mathrm{Im}[G(\omega)T(\omega)]$ for $T(\omega)$ and $G(\omega)$ as given by Eqs. (5), (6), and (10) with $\delta = -20\ s^{-1}$. This curve must encircle the point $(-V_o/\bar{P}_{inj},0)$ twice anticlockwise if perturbations are to decay with time. It is evident from the figure that perturbations decay, for some values of $V_o\bar{P}_{inj}$, for τ in the range $2.9 \le \tau \le 4.9$ ms. The optimum case occurs when the time delay across the feedback circuit is about 3.9 ms. Then, provided that $\bar{p}_{inj}$ is sufficiently large that $V_o/\bar{P}_{inj} < 4$, oscillations decay with their amplitudes decreasing until $V_o/\bar{P}_{inj} = 1$. Perturbations with $V_0/\bar{P}_{inj} < 1$ grow, and hence $V_o/\bar{P}_{inj} = 1$ describes a stable limit cycle. In dimensional terms, this limit cycle has an amplitude $v_o = \bar{p}_{inj}/420$ kPa. Since the amplitude of this limit cycle increases as $\bar{p}_{inj}$ is increased, we call it the "feedback mode."

Results for other negative values of δ are similar. As $-\delta$ is increased, the uncontrolled system has a larger growth rate than for the case shown in Fig. 6. The corresponding Nyquist curves then show a reduction in the range of τ that can be used to stabilize the flame. Nevertheless, the predicted optimum time delay is virtually unchanged. This is convenient because, as we have already noted, the precise value of δ is not known when the control circuit is being designed. These calculations have shown that a feedback circuit with a time delay of about 3.9 ms should be built.

The effect of the time delay across the feedback circuit on the measured pressure band level (PBL) in the range 0–400 Hz at $x = 0.725$ m is shown in Fig. 7. It can be seen that the theoretical optimum value of 3.9 ms agrees well with the time delay that leads to a maximum reduction in the measured PBL. Data in Fig. 7 are for two values of the mean back pressure to the injectors, $\bar{p}_{inj}$. At the higher value of $\bar{p}_{inj}$, a significant reduction in PBL occurs over a wider range of delay times. When $\bar{p}_{inj}$ is reduced, the data become more scattered and the range of delays over which a reduction in sound is possible is smaller. The experimentally determined optimum delay is near 3.5 ms and values in the range 3.4–3.6 ms have been used in the remaining experiments.

The Nyquist curves in Fig. 6 showed that an increase in $\bar{p}_{inj}$ increases the range of initial amplitudes of oscillation that can be controlled. But it also leads to an increase in the magnitude of the feedback mode. This can be seen clearly in the experimental results in Fig. 8 for a time delay of 3.4 ms. The primary equivalence ratio was kept constant at 0.68 in these tests. No secondary fuel is added when the control is off. The uncontrolled spectra in Fig. 8 show a narrow band peak near 74 Hz due to a combustion instability. We call this the "buzz" mode. "Control on" involves the unsteady injection of secondary fuel and hence a higher total fuel-air ratio. For this value of time delay, it is seen that as $\bar{p}_{inj}$ is increased, the frequency of the buzz mode is gradually altered and its amplitude is reduced. We call this peak the "modified buzz" mode. However, as $\bar{p}_{inj}$ is increased, a second peak due to the feedback mode begins to appear. The optimum for our control system is approximately $\bar{p}_{inj} = 333$ kPa. If $\bar{p}_{inj}$ is increased above this, the feedback mode becomes significantly large. A more sophisticated control circuit is required for complete stability. We have not pursued this further optimization. Our aim has been simply to demonstrate that the unsteady addition of fuel is a suitable way of implementing the feedback and that the performance of such a controller can be predicted from simple control theory.

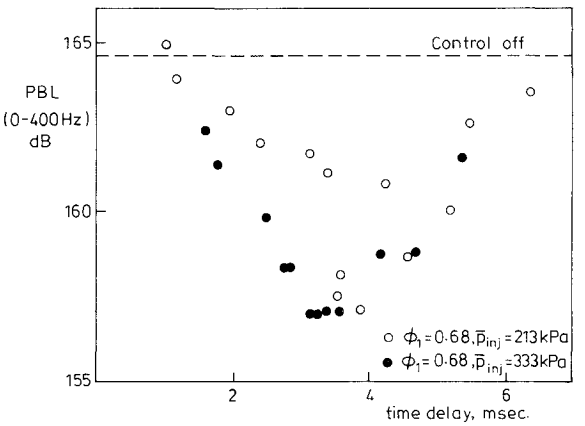

Fig. 7 The effect of the time delay across the feedback circuit on the measured pressure-band level in the range 0–400 Hz for two values of $\bar{p}_{inj}$. The PBL without control is shown by the dashed line.

The origin of the two low-frequency peaks in the controlled spectrum can be further illustrated by examining the Rayleigh source term at these frequencies. This source term has been written down by Chu[19] and is

$$\int_0^L \frac{(\gamma-1)}{\bar{\rho}\bar{c}^2}\overline{q'p'}\,dx \tag{14}$$

where $\bar{\rho}$ is the local mean density, $\bar{c}$ the local mean sound speed, q' the fluctuating component of heat-release rate per unit length, p' the fluctuating component of pressure, and the overbar denotes a short time average over one period of the oscillation. If the integral in Eq. (14) is negative, it indicates

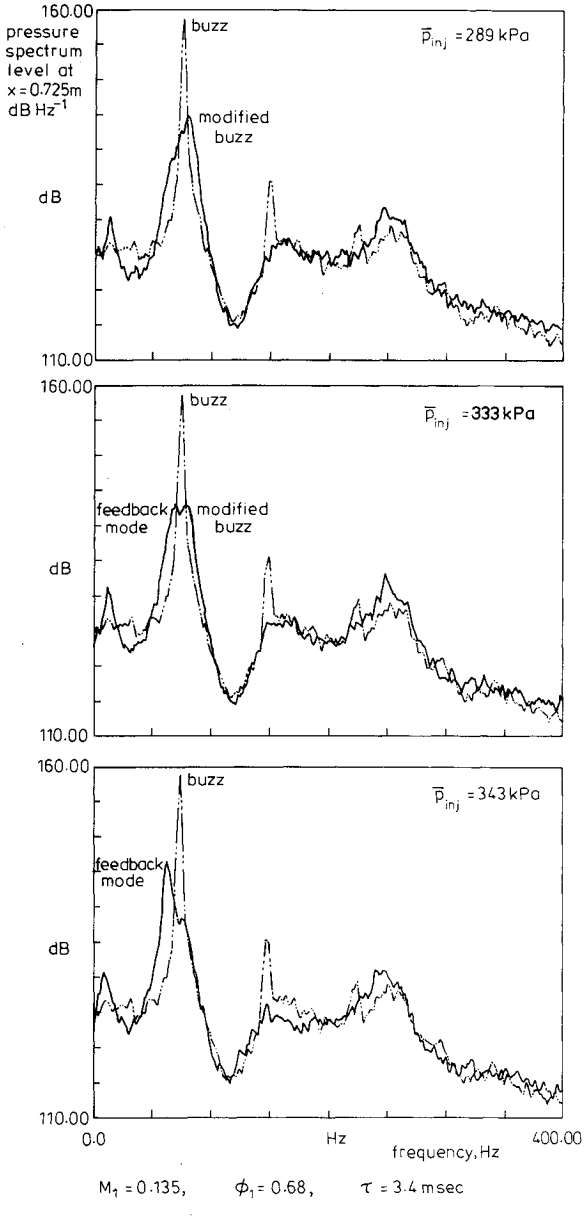

Fig. 8 The effect of an increase in the injector back pressure $\bar{p}_{inj}$ on the pressure spectrum level upstream of the flame. Dotted curves are spectra without control while solid curves show the effect of control.

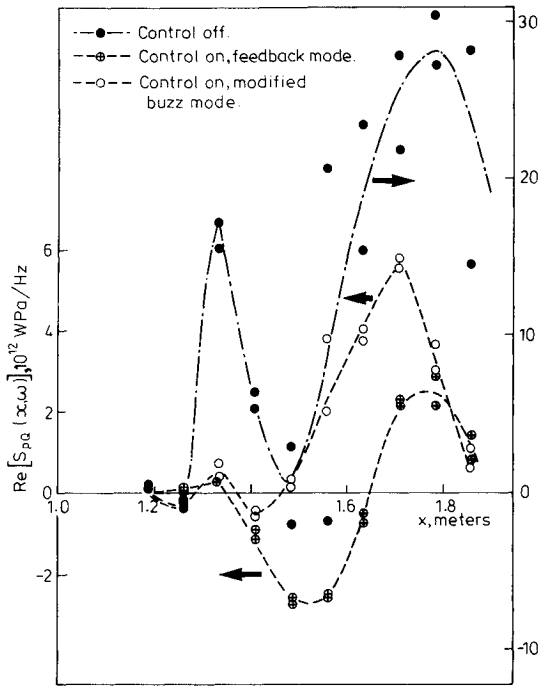

Fig. 9 The cross-power spectral density of $p(x,t)$ and $Q(x,t)$ plotted as a function of axial position for the buzz mode without control and for the modified buzz and feedback modes with control for the running conditions in Table 1.

that, on average, the acoustic disturbances are damped by the unsteady combustion and the system is stable. When it is positive, however, disturbances gain energy from the combustion. If this energy gain is greater than that lost on reflection at the boundaries, linear perturbations will be unstable.

The contribution to the Rayleigh source term from a 75-mm-long window centered on x is proportional to $\overline{Q'(x,t)p'(x,t)}$, where $Q'(x,t)$ is the unsteady heat-release rate within the window. This can be expressed in terms of $S_{pQ}(x,\omega)$, the cross-power spectral density between $p(x,t)$ and $Q(x,t)$. From the definition of cross-power spectral density,

$$\overline{Q'(x,t)p'(x,t)} = \frac{1}{2\pi}\int_{-\infty}^{\infty} S_{pQ}(x,\omega)\,d\omega = \frac{1}{\pi}\int_{0}^{\infty} \mathrm{Re}[S_{pQ}(x,\omega)]\,d\omega \qquad (15)$$

since $S_{pQ}(x,-\omega) = S^*_{pQ}(x,\omega)$. The function $\mathrm{Re}[S_{pQ}(x,\omega)]$ can be calculated from two sets of transfer functions. We denote the transfer functions between the pressure at axial positions x along the duct and the reference pressure by $\hat{p}(x,\omega)/\hat{p}_{ref}(\omega)$. These can be measured in a straightforward way. Similarly, the transfer functions $\hat{Q}(x,\omega)/\hat{p}_{ref}(\omega)$ have been obtained. Now

$$\mathrm{Re}[S_{pQ}(x,\omega)] = \left|\frac{\hat{p}(x,\omega)}{\hat{p}_{ref}(\omega)}\right| \left|\frac{\hat{Q}(x,\omega)}{\hat{p}_{ref}(\omega)}\right| \cos\Delta\theta S_p(\omega) \qquad (16)$$

The quantity $\mathrm{Re}[S_{pQ}(x,\omega)]$ has been calculated for each window at the buzz frequency without control and at the frequencies of both the feedback mode and the modified buzz mode with control. The results are plotted in Fig. 9. When Re $[S_{pQ}(x,\omega)]$ is multiplied by $(\gamma-1)/\bar{\rho}\bar{c}^2$, it gives the contribution to the Rayleigh source term from disturbances of frequency ω in the window centered on x. The product $(\gamma-1)/\bar{\rho}\bar{c}^2$ only changes by about 3% along the duct and this variation will be ignored. Hence, when data for each frequency in Fig. 9 are summed along the duct, they indicate the net energy gained from the combustion by acoustic disturbances.

It is apparent from Fig. 9 that without control the Rayleigh source term is large and positive at the buzz frequency. This source term is clearly reduced in amplitude when the controller is switched on (note the change of scale). However, it is undoubtedly still positive at the higher of the two frequencies indicating some driving from the combustion. This is the disturbance we have identified as the modified buzz mode. At the lower frequency, there is little net destabilizing contribution along the duct. This mode is at such a frequency that it is augmented by the addition of fuel with the time delay required to cancel the buzz frequency. We have called this the feedback mode.

Figure 8 illustrates that the application of control has significantly reduced the sharp peak in the uncontrolled pressure spectrum. Table 1 summarizes the performance of the controller for the case $\bar{p}_{inj}=333$ kPa. With the total airflow rate and the primary equivalence ratio constant, the addition of 3% more fuel has reduced the PBL within 3 dB of the peak at the buzz frequency by at least 12 dB. In the range 0-400 Hz, the controlled acoustic power is reduced to 18% of its uncontrolled value. As well as the reductions in sound level, there is an increase of 10% in the gauge pressure Δp upstream of the

Table 1 Results

	Control on			
	Feedback	Modified buzz	Control off	Change
Frequency, Hz	65	80	74	—
Δp, kPa	6.95		6.28	10%
M_1, kgs^{-1}	0.135		0.135	—
ϕ_1	0.68		0.68	—
M_2, kgs^{-1}	10×10^{-3}		10×10^{-3}	—
ϕ_2	0.28		—	—
M_T, kgs^{-1}	0.145		0.145	—
ϕ_T	0.65		0.63	3%
$\bar{p}_{inj}$, kPa	333		—	—
τ, ms	3.6		—	—
$\bar{m}_{f2}/m_{f1}$	3%		—	—
PBL (−3 dB of peak), dB at $x=0.75$ m	151.6	152.0	164.1	−12.5 −12.1
PBL (0–400 Hz), dB at $x=0.75$ m	157.2		164.6	−7.4
Controlled acoustic power / Uncontrolled acoustic power (0–400 Hz)	—		—	18%

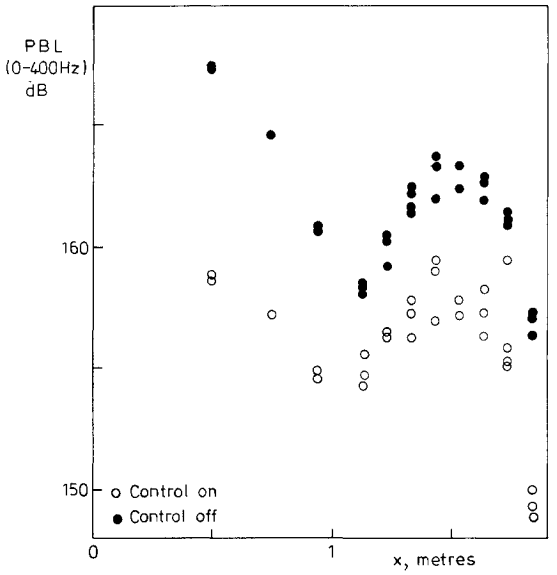

Fig. 10 Pressure-band level over 0–400 Hz plotted as a function of axial position with and without control for the running conditions in Table 1.

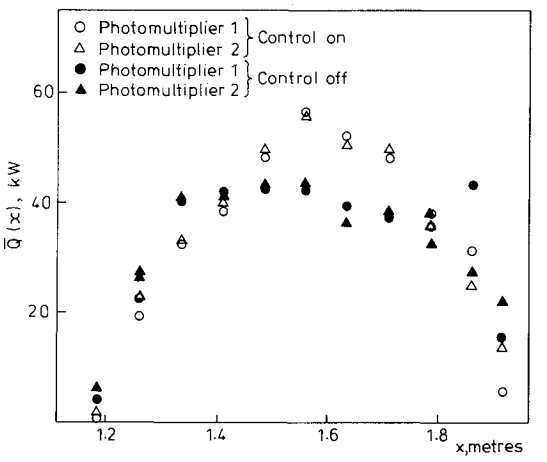

Fig. 11 The axial distribution of mean heat-release rate with and without control for the running conditions in Table 1.

flame. This indicates that more combustion occurs within the duct when controller is on.

In Table 1, we have only considered the effect of applying active control on the broadband sound power at the reference position. The PBL over the bandwidth 0–400 Hz along the entire working section is shown in Fig. 10. The application of active control reduces the PBL at all locations in the duct, despite the changes in frequency and mode shape.

Figure 11 shows that the application of control changes the axial distribution of mean heat-release rate, as well as increasing its overall level due to the increase in ϕ_T. Without control the mean heat-release rate has a maximum close to the gutter lip and then decreases. This is characteristic of a highly perturbed flame.[14] The application of control moves the maximum in mean heat-release rate downstream, a characteristic of a more stable flame.

So far the comparison has been made with an uncontrolled case in which the secondary fuel is switched off, $m_{f2}=0$; an example of case 1 in our classification. When the control is on, secondary fuel is added unsteadily, while M_1, ϕ_1, and m_{a2} are held at the same constant values as in the no-control case. This results in an increase in ϕ_T and leads to the question of how the controlled case compares with alternative fueling schemes for the same overall equivalence ratio. The same value of ϕ_T could be achieved by adding more primary fuel or by the steady injection of secondary fuel as in case 2. Figures 12–14 display the results of a parametric study of the response of the system to the various alternative methods of fuel injection.

Figure 12 shows data collected by injecting the secondary mass flow as in cases 1, 2, and 4 above, and plotting buzz frequency against ϕ_T. As we have seen in Fig. 8 for case 4 when the control is on, there are two frequencies at each value of ϕ_T. Clearly, the data for the modified buzz frequency, along with that for cases 1 and 2, show that the buzz frequency is determined primarily by the total equivalence ratio rather than the location at which fuel is added. As we might expect, the feedback frequency is anomalous in this figure.

In contrast to the frequency, Fig. 13 shows that the stability of the flame/duct configuration with steady fueling is influenced by the proportions of primary and secondary fuel which result in a given ϕ_T. Curves are drawn through points at a constant value of ϕ_1, with ϕ_T being increased by the steady addition secondary fuel. For example, all values of PBL are higher for $\phi_1=0.67$ than they are for $\phi_1=0.65$, despite the fact that there is region where the values of ϕ_T overlap. Therefore, this diagram shows that addition of fuel at the location of the

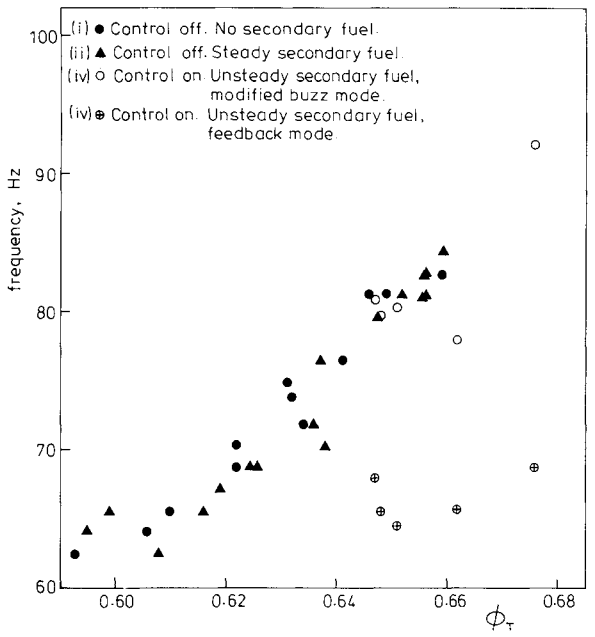

Fig. 12 The effect of the total fuel-to-air ratio on the dominant frequency. Data are shown for various methods of fuel addition.

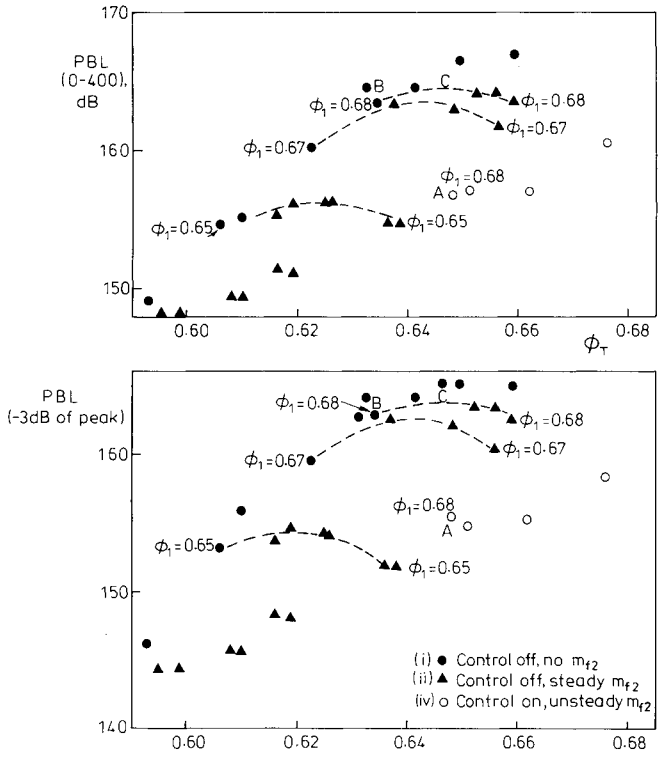

Fig. 13 The effect of the total fuel-to-air ratio on the pressure-band level within 3 dB of the peak and on the pressure-band level over 0–400 Hz. Dashed curves are drawn through data at constant ϕ_1. Fuel is added to the system by various methods.

secondary injectors is less destabilizing than mixing the same amount into the primary flow.

In Table 1, we compared results at the same ϕ_1 with $m_{f2}=0$ in the no-control case. An alternative test for the effectiveness of the controller would be to compare results for the same ϕ_1 and ϕ_T with and without control. In this comparison, the no-control case would involve the steady addition of

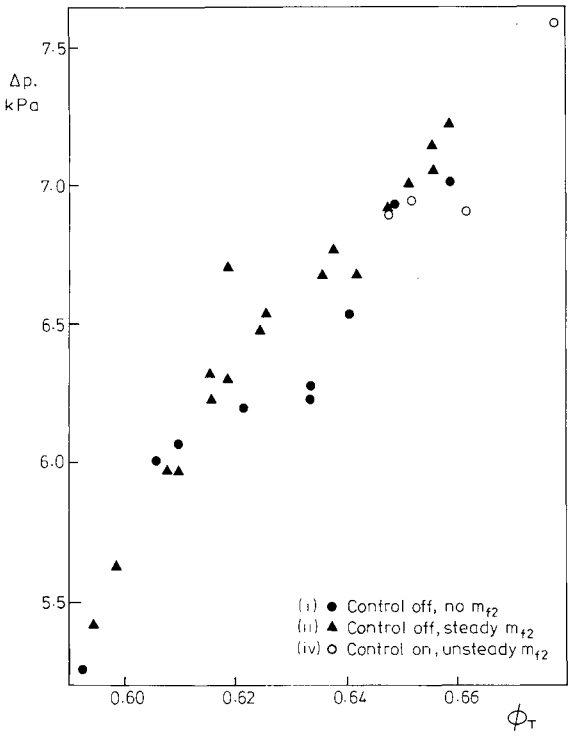

Fig. 14 The effect of total fuel-to-air ratio on Δp, the gauge pressure upstream of the flame, for various methods of fuel addition.

secondary fuel to give the same value of m_{f2} as when the controller is switched on. For example, the controlled case for $\phi_1=0.68$ (point A on Fig. 13) is compared with point B in Table 1. If the comparison is performed at constant ϕ_1 and ϕ_T, then the effectiveness of the controller would be measured as the difference between point A and point C. It is apparent from Fig. 13 that these two different comparisons lead to no appreciable difference between the measured effectiveness of the controller.

We saw in Table 1 that Δp, the gauge pressure just upstream of the flame, increased by 10% when the controller was switched on. This means that more heat is released within the duct and the thrust is increased. Figure 14 explains why this occurs. It shows Δp to be roughly proportional to the overall equivalence ratio ϕ_T and that a similar improvement in thrust can be made by the steady addition of fuel. The main advantage of the controller is also illustrated in this figure. It enables a flame to burn in the rig at a higher fuel-air ratio than is possible without control. This results in an increase in the maximum available thrust.

Conclusions

Combustion oscillations in an 0.25-MW burner can be stabilized by the unsteady addition of extra fuel. The required characteristics of the controller can be predicted from measured transfer functions describing the flame's response. A suitably phased addition of 3% more fuel reduces the 164 dB peak in the pressure spectrum due to the combustion oscillations by about 12 dB. The acoustic energy in the 0–400 Hz bandwidth is reduced to 18% of its uncontrolled value. The controller enables the rig to run at high fuel-air ratios at which it is impossible to stabilize a flame without control. This leads to an increase in the maximum available thrust.

The control system exploits the chemical energy in the fuel to alter the acoustic energy balance in the duct. Relatively little mechanical power is needed to produce the required unsteady fuel injection. Hence, this method of feedback has considerable potential for full-scale applications.

Acknowledgments

This project was funded by Rolls-Royce and was carried out at the Whittle Laboratory, Cambridge University Engineering Department, while P. J. Langhorne was the Rolls-Royce Research Fellow in Engineering at Newnham College. The authors thank A. Sotheran and J. Lewis of Rolls-Royce for their stimulating interest in this work.

References

[1]Smart, A. E., Jones, B., and Jewell, N. T., "Measurements of Unsteady Parameters in a Rig Designed to Study Reheat Combustion Instabilities," AIAA Paper 76-1141, 1976.

[2]Rayleigh, J. W. S., *The Theory of Sound: Vol. II*, No. 8, Dover, New York, 1945.

[3]Collyer, A. A., and Ayres, D. J., "The Generation of Sound in a Rijke Tube Using Two Heating Coils," *Journal of Physics D.*, Vol. 5, 1972, pp. L73-L75.

[4]Heckl, M. A., "Heat Sources in Acoustic Resonators," Ph.D. Thesis, Cambridge Univ., Cambridge, England, U.K., 1985.

[5]Screenivasan, K. R., Raghu, S., and Chu, B. T., "The Control of Pressure Oscillations in Combustion and Fluid Dynamical Systems," AIAA Paper 85-0540, March 1985.

[6]Dines, P. J., "Active Control of Flame Noise," Ph.D. Thesis, Cambridge Univ., Cambridge, England, UK, 1983.

[7]Hurle, I. R., Price, R. B., Sugden, T. M., and Thomas, A., "Sound Emission from Open Turbulent Premixed Flames," *Proceedings of the Royal Society of London*, Ser. A, Vol. 303, Royal Society, London, 1968, pp. 409-427.

[8]Heckl, M. A., "Active Control of the Noise from a Rijke Tube," *IUTAM Symposium on Aero and Hydro-Acoustics, Lyon 1985*, Springer-Verlag, Berlin, 1986.

[9]Kidin, N., Librovich, V., Medvedev, N., Roberts, J., and Vuillermoz, M., "An Anti-Sound Technique for Controlling Combustion System Instabilities," Workshop on Gas Flame Structure, Novosibirsk, 1986.

[10]Lang, W., Poinsot, T., and Candel, S., "Active Control of Combustion Instability," *Combustion and Flame*, Vol. 70, 1987, pp. 281-289.

[11]Poinsot, T., Bourienne, F., Eposito, E., Candel, S., and Lang, W., "Suppression of Combustion Instabilities by Active Control," AIAA Paper 87-1876, June 1987.

[12]Bloxsidge, G. J., Dowling, A. P., Hooper, N., and Langhorne, P. J., "Active Control of an Acoustically Driven Combustion Instability," *Journal of Theoretical and Applied Mechanics*, (Suppl.) Vol. 6, 1987, pp. 161-175.

[13]Bloxsidge, G. J., Dowling, A. P., Hooper, N., and Langhorne, P. J., "Active Control of Reheat Buzz," *AIAA Journal*, Vol. 26, No. 7, 1988, pp. 783-790.

[14]Langhorne, P. J., "Reheat Buzz—An Acoustically Coupled Combustion Instability, Part 1: Experiment," *Journal of Fluid Mechanics*, Vol. 193, 1988, pp. 417-443.

[15]Bloxsidge, G. J., Dowling, A. P., and Langhorne, P. J., "Reheat Buzz—An Acoustically Coupled Combustion Instability, Part 2: Theory," *Journal of Fluid Mechanics*, Vol. 193, 1988, pp. 445-473.

[16]Norbye, J. P., *Automotive Fuel Injection Systems—A Technical Guide*, Haynes, England, 1982.

[17]Ogata, K., *Modern Control Engineering*, Prentice-Hall, Englewood Cliffs, NJ, 1970.

[18]Dorf, R. C., *Modern Control Systems*, Addison-Wesley, Reading, MA, 1980.

[19]Chu, B. T., "On the Energy Transfer to Small Disturbances in Fluid Flow (Pt. I)," *Acta Mechanica*, Vol. 1, 1964, pp. 215-234.